γ-ray spectroscopy of the odd-odd $N = Z + 2$ deformed proton emitter ^{112}Cs

P. T. Wady,[1,2] J. F. Smith,[1,2,*] E. S. Paul,[3] B. Hadinia,[1,2,†] C. J. Chiara,[4,‡] M. P. Carpenter,[5] C. N. Davids,[5] A. N. Deacon,[6] S. J. Freeman,[6] A. N. Grint,[3] R. V. F. Janssens,[5] B. P. Kay,[6,§] T. Lauritsen,[5] C. J. Lister,[5] B. M. McGuirk,[3] M. Petri,[3,‖] A. P. Robinson,[5,¶] D. Seweryniak,[5] D. Steppenbeck,[6,**] and S. Zhu[5]

[1]*School of Engineering, University of the West of Scotland, Paisley PA1 2BE, United Kingdom*
[2]*Scottish Universities Physics Alliance (SUPA)*
[3]*Oliver Lodge Laboratory, University of Liverpool, Liverpool L69 7ZE, United Kingdom*
[4]*Department of Chemistry, Washington University, St. Louis, Missouri 63130, USA*
[5]*Physics Division, Argonne National Laboratory, Argonne, Illinois 60439, USA*
[6]*School of Physics and Astronomy, University of Manchester, Manchester M13 9PL, United Kingdom*

(Received 1 December 2011; published 23 March 2012)

Gamma-ray transitions have been observed in the proton-emitting $N = Z + 2$ ($T_z = 1$) isotope ^{112}Cs. The transitions have been unambiguously assigned to ^{112}Cs by correlation with the characteristic proton decay, using the method of recoil-decay tagging with mass selection. The measured proton-decay energy and half-life are $E_p = 810(5)$ keV and $T_{1/2} = 470(50)$ μs, respectively, which are consistent with previous measurements. Five γ-ray transitions have been observed which appear to form a rotational sequence. The energy differences between excited states in the sequence are consistent with an assignment as the favored signature of the $\nu(h_{11/2}) \otimes \pi(h_{11/2})$ structure. Tentative evidence for fine structure in the ^{112}Cs proton decay is also observed.

DOI: 10.1103/PhysRevC.85.034329 PACS number(s): 23.20.Lv, 23.50.+z, 27.60.+j, 29.30.Kv

I. INTRODUCTION

One of the important themes in present-day nuclear-structure physics is the study of nuclei at, and beyond, the particle drip lines. This interest has been motivated by calculations which suggest that structural properties may change significantly with a severe imbalance of neutrons and protons compared to stable isotopes [1]. In the $A = 110$ region, the locus of nuclei having $N = Z$ and the proton drip line lie in very close proximity to each other. Odd-odd nuclei with $N \simeq Z$ are particularly interesting to study since the unpaired neutron and proton will occupy similar orbitals with a large spatial overlap in their wave functions. The very neutron-deficient $Z = 55$ cesium isotopes, near and at the proton drip line, are well deformed with quadrupole deformation parameters of $\beta_2 \simeq 0.25$ [2–4]. The rotational properties of these nuclei, such as quasiparticle alignment frequencies and moments of inertia, can be used to characterize intrinsic states and infer structural information. The cesium isotopes with $A \leqslant 120$ have both their neutron and proton Fermi levels located within the $h_{11/2}$ subshells. With $Z = 55$ and $\beta_2 \simeq 0.25$, the proton Fermi level lies close to the $[550]1/2^-$ orbital, and as N approaches 55, the neutron Fermi level moves toward the low-Ω $h_{11/2}$ orbitals. As a consequence, the spatial overlap of the unpaired neutron and proton increases with decreasing N, resulting in an increased neutron-proton (np) interaction, with associated structural consequences [4,5].

Experimental study of the exotic neutron-deficient nuclei around $A = 110$ is challenging. The best way to produce these nuclei in the laboratory is to use heavy-ion fusion-evaporation reactions with the most neutron-deficient beams and targets available. However, when the compound nuclei themselves are very neutron deficient, the evaporation of α particles and protons is energetically favored over neutron emission, which often leads to a large number of product nuclei. Furthermore, the relatively low probability for neutron evaporation means that the most neutron-deficient reaction products have some of the smallest cross sections. The residues of neutron evaporation are, therefore, produced among a large number (often around 15 to 20) of other, far more intense, products. In order to study the most neutron-deficient products, highly selective methods of channel selection and identification are essential. Recoil-decay tagging (RDT) [6] has become a well-known method of channel selection and identification in γ-ray spectroscopy. In essence, the RDT method involves three steps: (i) detection of γ rays at the reaction site, (ii) implantation of the recoiling reaction products into a highly segmented silicon detector at the focal plane of a recoil separator, and (iii) measurement of the decay characteristics of the implanted nuclei (energies and times). Using spatial and temporal correlations of characteristic decays and implanted reaction products, together with the coincidence of implanted products and detected γ rays, it is possible to identify the isotopic origin of the γ-ray transitions unambiguously.

*john.f.smith@uws.ac.uk
†Present address: Department of Physics, University of Guelph, Guelph, Ontario, N1G 2W1, Canada.
‡Present address: Department of Chemistry and Biochemistry, University of Maryland, College Park, Maryland 20742, USA.
§Present address: Department of Physics, University of York, Heslington, York YO10 5DD, United Kingdom.
‖Present address: Lawrence Berkeley National Laboratory, Berkeley, California 94720, USA.
¶Present address: School of Physics and Astronomy, University of Manchester, Manchester M13 9PL, United Kingdom.
**Present address: RIKEN Nishina Center, 2-1, Hirosawa, Wako, Saitama 351-0198, Japan.

Proton and α decay of nuclei in the neutron-deficient $A = 110$ region was first observed over 25 years ago [7–9]. There is now a well-established island of α-particle- and proton-emitting nuclei in this region. In the past 10 years, these characteristic decay properties have been exploited in RDT experiments to study the structure of nuclei which were hitherto inaccessible in γ-ray spectroscopy experiments. For example, excited states have recently been identified and studied in $^{106-109}_{52}$Te [6,10,11], $^{109}_{53}$I [6,12,13], $^{110}_{54}$Xe [14], and $^{113}_{55}$Cs [15]. To date, no information about the excited states of ^{112}Cs has been available. The decay properties of $^{112}_{55}$Cs were studied by Page *et al.* [16]; in that work, the ground state was shown to decay by proton emission with energy 807(7) keV, and half-life of 500(100) μs. The ^{112}Cs nuclei were produced using the ^{58}Ni(^{58}Ni,$p3n$) reaction, with a reported cross section of $\sim$500 nb [16]; this reaction remains the only viable current method by which to produce ^{112}Cs. As reported in Ref. [16], the proton-emitting isotopes $^{109}_{53}$I ($\alpha p2n$ evaporation) and $^{113}_{55}$Cs ($p2n$) are also produced in this reaction and with significantly larger cross sections than that for ^{112}Cs. Furthermore, the proton-decay properties of ^{109}I are very similar to those of ^{112}Cs: In Ref. [13], and references therein, the proton-decay energy and half-life of ^{109}I are reported to be 813(4) keV and 92(1) μs, respectively. Therefore, any experiment designed to study ^{112}Cs using the RDT method will be challenged by the simultaneous production of ^{109}I.

The neutron-deficient cesium isotopes with $A \geqslant 118$ can be produced with relatively large cross sections and have been studied well in γ-ray spectroscopy experiments. Below $A = 118$, the production cross sections, and, consequently, the quality of experimental data available for each nucleus, reduce with decreasing neutron number. Thus, in odd-odd ^{118,120}Cs ($N = 63, 65$), multiple high-spin two-quasiparticle rotational bands have been identified [3,17–20]. For ^{116}Cs ($N = 61$), just one rotational band has been observed, assumed to be built on the yrast $\nu(h_{11/2}) \otimes \pi(h_{11/2})$ configuration [21]. Recently, in ^{114}Cs ($N = 59$), a sequence of around six γ-ray transitions has been identified, which is assigned to form the favored-signature sequence of the yrast $\nu(h_{11/2}) \otimes \pi(h_{11/2})$ configuration [22]. In the present work, an experiment was performed to identify and study γ-ray transitions from the decay of excited states in ^{112}Cs, using the RDT method. Five (tentatively six) γ-ray transitions have been observed and assigned to this nucleus.

II. EXPERIMENTAL DETAILS

The ^{58}Ni(^{58}Ni,$p3n$) reaction used by Page *et al.* [16] was shown to produce ^{112}Cs; the same reaction was used in the present work. A ^{58}Ni beam, with energy 260 MeV and intensity $\sim$9 pnA, was provided by the ATLAS accelerator system at Argonne National Laboratory. The beam was incident on a thin, self-supporting ^{58}Ni target with a thickness of 565 μg/cm^2. Gamma rays emitted at the reaction site were detected using the Gammasphere spectrometer [23,24]. Gammasphere is an array of Compton-suppressed high-purity germanium detectors arranged in 17 rings of constant polar angle θ with respect to the beam axis. In the present work, 101 detectors were used. After the target, recoiling reaction products were dispersed according to their mass-to-charge-state ratio (A/q) by the Argonne Fragment Mass Analyzer (FMA) [25,26], before being detected by a parallel-grid avalanche counter (PGAC) at the focal plane and subsequently implanted into a double-sided silicon strip detector (DSSD). The FMA was set up such that evaporation residues with mass numbers $108 \lesssim A \lesssim 116$ and charge states $25 \leqslant q \leqslant 27$ were transported to the focal plane. The DSSD had an area of 32×32 mm^2 and a thickness of 60 μm. It was divided into eighty 400-μm-wide strips in each of the horizontal and vertical directions on the front and back, respectively, resulting in 6400 effective pixels. Data were recorded when either one of two trigger conditions was satisfied: (i) when any signal was recorded in the DSSD or (ii) when 13 or more unsuppressed γ rays were detected in coincidence by Gammasphere. For the results presented here, only the data triggered by the DSSD were used. All of the recorded events included a 47-bit time stamp from a continuously running 1-MHz clock, enabling the absolute time of each event to be known to the nearest microsecond. This microsecond clock was used throughout this analysis to identify implant-decay time correlations.

It was expected that around 15 to 20 different evaporation residues would be produced in the reaction, most of which would have cross sections considerably larger than that of ^{112}Cs. Furthermore, several of these residues decay by α-particle or proton emission, which complicate the RDT analysis. In order to prevent unwanted evaporation residues from being implanted into the DSSD, "mass slits" were introduced into the path of the residues immediately before the PGAC at the focal plane of the FMA. These slits were positioned to stop all residues with $A \neq 112$, thereby reducing the overall implant rate in the DSSD and lowering the rate of successive implants in any one pixel. The slits were set up to allow residues with A/q values of either 112/27 or 112/26 to reach the focal plane, resulting in an A/q spectrum consisting of two separated peaks on flat (zero) background. However, despite the use of the slits, overlapping A/q values and the tails of neighboring A/q peaks remained issues to be addressed.

III. DATA ANALYSIS AND RESULTS

A. Gamma-ray coincidence data and reaction products

The beam irradiated the target for around 110 h, during which time approximately 90 GB of data were written to disk. In total, 1.2×10^9 events were recorded; 5.5×10^8 of the events (46%) were triggered by the DSSD. Overall, the γ-ray coincidence data had a mean suppressed γ-ray fold of 9, while the data triggered by the DSSD had a mean fold of 6. The off-line analysis was carried out with one-, two-, and three-fold γ-ray events (*single*, *double*, and *triple events*). As a starting point in the analysis, two-dimensional histograms (*matrices*) and three-dimensional histograms (*cubes*) were created from the unfolded double and triple events; unfolding resulted in a total of 1.7×10^{10} double and 3.7×10^{10} triple events. The spectra were analyzed using the codes GF3, ESCL8R and LEVIT8R [27], and DATA-VIEW [28]. Analysis of the ungated (no recoil condition) γ-ray spectra revealed that excited states were

populated in at least 20 evaporation residues, with the most intense being ^{112}Te ($4p$ evaporation), ^{111}Te ($4pn$), ^{110}Te ($\alpha 2p$), ^{109}Sb ($\alpha 3p$), ^{109}Te ($\alpha 2pn$),^{113}I ($3p$), ^{112}I ($3pn$), and ^{111}Sb ($5p$). In the spectra that were incremented in coincidence with a signal in the PGAC, γ rays from ^{112}Te and ^{112}I dominated, with peaks due to $A \neq 112$ residues reduced significantly, clearly illustrating the effectiveness of the mass slits. A comparison of γ-ray intensities in spectra incremented by events with γ-ray fold $\geqslant$13 (suppressed), with and without the requirement of a recoil detected by the PGAC, indicated that the FMA transmission efficiency was between 5% and 10%.

B. Recoil-decay tagging

The first step in the RDT analysis was to identify and select the signals recorded by the DSSD that correspond to ^{112}Cs proton decays. The best method to achieve this goal was to study the relationship between the horizontal position of residues in the PGAC (proportional to A/q) and the decay energy. A two-dimensional spectrum of these parameters is given in Fig. 1. The spectrum is incremented when decays occur within 1500 μs of the implant into the DSSD. With a half-life of 500(100) μs [16], this time condition will include $\sim$90% of the ^{112}Cs decay events in the spectrum, while eliminating any longer-lived decays. The spectrum in Fig. 1 clearly exhibits two distinct groups of counts, a lower group and an upper group, corresponding to the A/q values of 112/27 and 112/26, respectively. In the lower (112/27) group, all of the counts appear to fall into one main region, whereas in the upper (112/26) group, the counts fall into three clusters. In order to identify the origin of these clusters, the A/q values were calibrated using the known positions of the 112/27 and

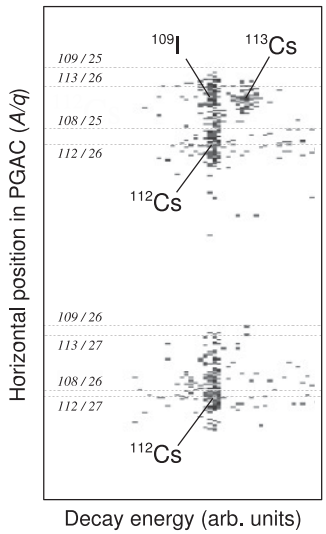

FIG. 1. Horizontal position in the PGAC, proportional to A/q, plotted against decay energy recorded in the DSSD. The data are collected into two main groups on the vertical axis: The lower group includes $A/q = 112/27$ and the upper group includes $A/q = 112/26$. The positions of nearby A/q values are marked by horizontal dashed lines. The clusters of data points corresponding to ^{109}I ($A/q = 109/25$) and ^{113}Cs ($A/q = 113/26$) are labeled.

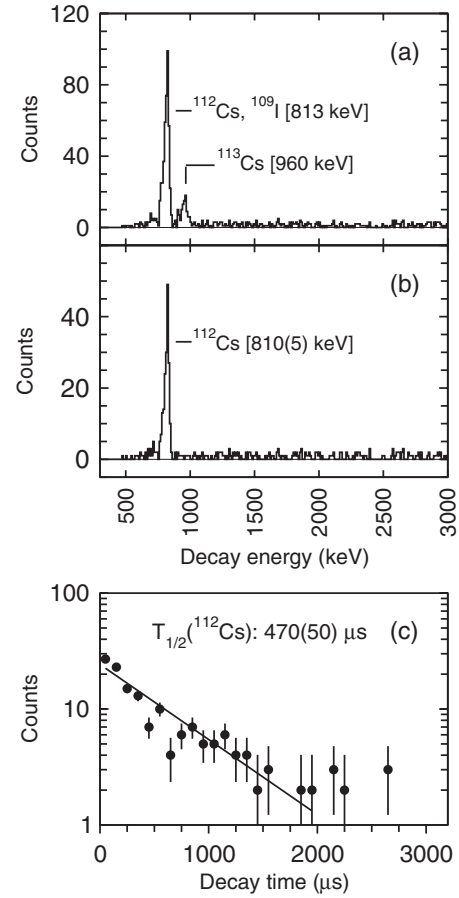

FIG. 2. Panels (a) and (b) give the energies recorded in the DSSD within 1500 μs of an implanted evaporation residue. Panel (a) is the spectrum recorded from all of the data; although the mass slits are in place, decays of ^{109}I and ^{113}Cs are also present due to overlapping A/q values. Panel (b) is the same spectrum but with a tighter restriction on A/q (horizontal PGAC position) in order to select only $A/q = 112/q$ residues. Panel (c) presents the time between implant in the DSSD and the decay event; the data are presented in 100-μs bins and are shifted by 70 μs to the left to account for the dead time of the data-acquisition system. The data in panel (c) are consistent with a half-life of 470(50) μs.

112/26 peaks. The upper two clusters of the 112/26 group lie close to A/q values of 113/26 and 109/25, and they have been assigned to ^{109}I ($E_p = 813(4)$ keV and $T_{1/2} = 92(1)$ μs [13]) and ^{113}Cs ($E_p = 959(6)$ keV [16] and $T_{1/2} = 18$ μs [15]). Further analysis of time differences between implants and decays supported these assignments.

Decay-energy spectra recorded by the DSSD are presented in Figs. 2(a) and 2(b). The spectra were incremented when a decay occurred within 1500 μs of an implant. For the spectrum in Fig. 2(a), no conditions were applied to the A/q values; the ^{113}Cs peak at 960 keV is clearly visible, and the large peak at $\sim$810 keV consists of counts due to both ^{112}Cs and ^{109}I decays. For the spectrum in Fig. 2(b), it was required that the A/q value of the decaying residue fell within either of the ^{112}Cs regions marked on Fig. 1. With this condition, the ^{113}Cs peak is eliminated completely. As the ^{113}Cs cluster lies at a slightly lower A/q value than the ^{109}I cluster (Fig. 1),

this suggests that the ^{109}I contribution to the large peak is also eliminated. Measurement of the energy of the ^{112}Cs decay peak in Fig. 2(b) gives a value of 810(5) keV, consistent with 807(7) keV measured in Ref. [16]. In order to measure the half-life of the ^{112}Cs proton decay, the times between implants and decays were studied. With tight selection of the $A = 112$ regions of A/q (Fig. 1) and on the ^{112}Cs decay energy [Fig. 2(b)], the times between implants and decays were grouped into bins of width 100 μs, and decay times up to 4 ms were considered. A logarithmic plot of these data is provided in Fig. 2(c). A straight-line fit to the data up to 1.6 ms gives a half-life value of 470(50) μs, which is consistent with that of 500(100) μs in Ref. [16]. The cross section for the production of ^{112}Cs in the present data has been estimated from the number of observed proton decays and accounting for detection efficiencies. The deduced cross section of 40(20) nb is considerably lower than the reported 500 nb value of Ref. [16]; the reason for this discrepancy is not clear.

C. Tentative fine structure in ^{112}Cs proton decay

An additional peak is observed in the decay-energy spectra which also appears to be associated with ^{112}Cs. This peak can be seen in Figs. 2(a) and 2(b), immediately to the left of the main ^{112}Cs decay. On Fig. 1, small clusters of counts are also visible on the left of the 112/27 and 112/26 clusters. These counts correspond to the decay of a residue with an A/q value consistent with assignment to ^{112}Cs. In the data analysis, various conditions have been set to test the validity and significance of this observation. In doing so, it has not been possible to eliminate the peak, and it must, therefore, be concluded that it has a real physical origin and is not an artifact of the analysis or of the low counting statistics. The energy of the peak is 710(20) keV, and it has around 10% of the intensity of the main ^{112}Cs decay peak. The half-life of the decay has been estimated, using the maximum-likelihood method [29,30], to be 170^{+50}_{-30} μs. This observation would represent fine structure in the proton decay of ^{112}Cs. If this is indeed a second proton decay in ^{112}Cs, then the energy difference between this decay and the known ^{112}Cs proton decay is 100 keV. This is interesting since the daughter nucleus $^{111}_{54}$Xe is known to decay by two α-decay branches with an energy difference close to 100 keV [7,8]. The two proton decays in ^{112}Cs may populate the ground and first-excited states in ^{111}Xe, which then decay by α-particle emission to the same state in $^{107}_{52}$Te. The α-decay chains $^{111}\mathrm{Xe} \rightarrow {}^{107}\mathrm{Te} \rightarrow {}^{103}\mathrm{Sn}$ and $^{109}\mathrm{Xe} \rightarrow {}^{105}\mathrm{Te} \rightarrow {}^{101}\mathrm{Sn}$ have recently been the subject of significant interest, since the observation of α decay of ^{105}Te to ^{101}Sn [31] and its fine structure [32] have given information about the first excited state in ^{101}Sn. However, with the low numbers of counts and large uncertainties in the present work, it is not possible to draw any definite conclusion about the states in ^{111}Xe.

D. Proton-correlated γ-ray transitions

In order to identify γ-ray transitions associated with the decay of excited states in ^{112}Cs, spectra were incremented with γ rays which were correlated with the characteristic

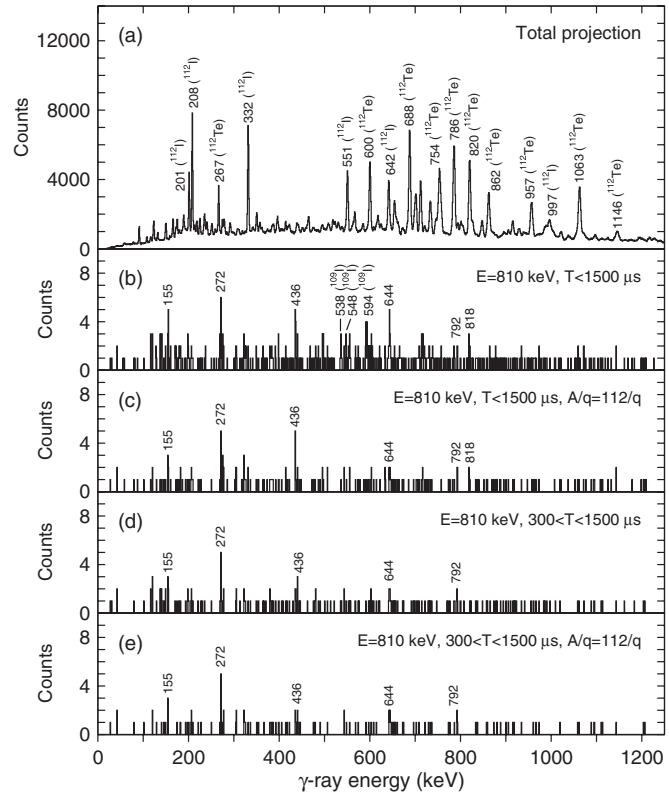

FIG. 3. Gamma-ray spectra recorded in this work. Panel (a) presents the projection of all γ rays which are detected in coincidence with a residue at the focal plane of the FMA; the largest peaks in the spectrum belong to nuclei with $A = 112$ (^{112}I and ^{112}Te, as labeled). Panel (b) shows γ rays correlated with proton decays of 810 keV within 1500 μs of an implant. The spectrum exhibits unknown transitions, which are assigned to the decay of excited states in ^{112}Cs, together with some known transitions in ^{109}I. Panel (c) is the same spectrum as panel (b), but with a tight condition on $A/q = 112/q$; the ^{109}I transitions are eliminated. Panels (d) and (e) are the same as panels (b) and (c), respectively, but with the additional condition that the decay occurs more than 300 μs after the implant, in order to eliminate decays of ^{109}I, which has a half-life of 100 μs. The additional condition for panel (d) clearly eliminates the ^{109}I transitions in panel (b).

^{112}Cs proton decays. Some γ-ray spectra resulting from this analysis are presented in Fig. 3. For comparison with the proton-correlated spectra, Fig. 3(a) gives the total projection of the γ-ray data collected in the experiment. All of the labeled peaks in the spectrum correspond to transitions in $^{112}_{52}$Te and $^{112}_{53}$I. The spectra in Figs. 3(b), 3(c), 3(d), and 3(e) are all correlated with 810-keV protons but have different correlation times and different A/q conditions. The spectrum in Fig. 3(b) is incremented when any decays occur within 1500 μs of the implant, but with no conditions on A/q. Four of the peaks observed in the spectrum, at 538, 548, 594, and 644 keV, can be assigned to transitions in ^{109}I which, with a half-life of 92(1) μs [13], will decay within the 1500-μs correlation time. The other peaks in the spectrum at 155, 272, 436, 792, and 818 keV do not belong to ^{109}I and are, therefore, assigned to the decay of excited states in ^{112}Cs. In order to eliminate the ^{109}I

TABLE I. Properties of γ-ray transitions assigned to ^{112}Cs. The column labeled E_γ gives the γ-ray energies in keV. The values $I_\gamma^{\rm meas}$ and $I_\gamma^{\rm corr}$ give the measured and corrected intensities. The right-hand column gives the assumed multipolarities of the transitions. For the 155- and 272-keV transitions, data are corrected for both $M1$ and $E2$ assignments.

E_γ (keV)	$I_\gamma^{\rm meas}$	$I_\gamma^{\rm corr}$	Mult.
154.6(0.6)	5(2)	6(3)	$M1$
272.1(1.2)	9(3)	12(4)	$M1$
435.6(0.6)	7(3)	12(4)	$E2$
643.7(1.0)	5(2)	10(5)	$E2$
792(1)	4(2)	9(5)	$E2$
818(1)	3(2)	7(4)	$E2$
154.6(0.6)	5(2)	7(3)	$E2$
272.1(1.2)	9(3)	12(4)	$E2$

γ rays from the spectrum, and to verify the assignment to ^{112}Cs, a condition was placed on A/q to select only the $112/q$ residues; the resulting spectrum is presented in Fig. 3(c). Three of the ^{109}I transitions in Fig. 3(b) are not present in Fig. 3(c), but the 644-keV peak is present with lower intensity. An alternative method to reduce the contribution from ^{109}I is to place a *lower* limit on the correlation time. The spectrum of Fig. 3(d) is incremented when residues decay between 300 and 1500 μs from the time of implant and with no A/q condition applied. With a half-life close to 100 μs, $\sim$90% of the ^{109}I residues will decay before 300 μs have elapsed. In Fig. 3(d), three of the ^{109}I transitions are eliminated, but the 644-keV transition again remains, albeit with a reduced intensity. Figure 3(e) gives the spectrum with both the A/q condition and with the 300-μs lower time limit; the transitions assigned to ^{112}Cs, with the exception of the 818-keV transition, still remain above the background in the spectrum. As a result of this analysis, the transitions assigned to the decay of excited states in ^{112}Cs have energies 155, 272, 436, 644, and 792 keV. The properties of these γ-ray transitions are summarized in Table I. The table gives the measured γ-ray energies together with relative intensities, both measured and corrected for detector efficiency and internal conversion, and possible multipolarity assignments.

IV. DISCUSSION

A. Level scheme

On the basis of the relative intensities of the γ-ray transitions, and a comparision with the level schemes of the neighboring heavier odd-odd cesium isotopes, a possible arrangement of the relative positions of excited states in ^{112}Cs is presented in Fig. 4. The presented level scheme assumes that the 436-, 644-, and 792-keV transitions have stretched $E2$ multipolarity, whereas the 272-keV transition is of $M1/E2$ character. The $M1/E2$ assignment to the 272-keV transition is primarily due to its lower energy but is also made on the basis of systematic comparison with ^{114}Cs. The relative intensities for the 272- and 155-keV transitions in Table I have been corrected under the assumption of both $E2$ and

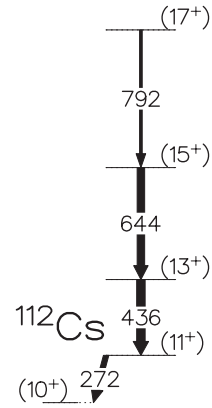

FIG. 4. The proposed level scheme of ^{112}Cs, deduced in this work. Transition energies are given in keV, with uncertainties of around 0.5 keV. The transitions have been ordered on the basis of intensity and by comparison to neighboring odd-odd cesium isotopes. Two transitions with energies 155 keV and, tentatively, 818 keV have been assigned to ^{112}Cs but are not placed in this level scheme.

$M1$ multipolarities. The intensity of the 272-keV transition does not appreciably differ whether correcting the intensity for either possibility. Although the 155-keV transition has been assigned to ^{112}Cs, it has not been placed in the level scheme. The 818-keV transition is not apparent in spectra with the 300-μs lower limit on the decay time, and it has, therefore, only been tentatively assigned to ^{112}Cs. The spin and parity assignments on Fig. 4 are made on the basis of systematic comparison with excitation energies of neighboring heavier cesium istopes, as discussed below, and are, therefore, tentative. In Ref. [33], the ground state of ^{112}Cs was proposed to have $I^\pi = 0^+$ or 3^+, through comparison of the measured proton-decay half-life with calculations. In the neighboring heavier odd-odd cesium isotopes ^{114,116,118}Cs, decay from the lowest observed state in the most intense rotational band to the ground state is not observed. This is presumably due to the low detection efficiency for low-energy transitions with the apparatus used [20–22]. In ^{120}Cs, decay of the 10^+ yrast band-head proceeds to the ground state by multiple low-energy, low-intensity transitions which were observed through the use of low-energy photon (LEPS) detectors [18]. It is possible that a similar arrangement of low-energy, low-intensity transitions will connect the states shown in Fig. 4 to the ^{112}Cs ground state. These transitions would be difficult to observe in the present work. Thus, the spin assignments proposed here are not inconsistent with the ground state J^π values proposed in Ref. [33].

B. Excitation-energy systematics and deformations

The neutron-deficient cesium isotopes are known to have well-deformed ground states. Figure 5(a) presents the calculated quadrupole deformation parameters β_2 for the odd-odd cesium isotopes with $55 \leqslant N \leqslant 71$ ($110 \leqslant A \leqslant 126$), taken from the macroscopic-microscopic approach of Möller, Nix, Myers, and Swiatecki [2], from the total-Routhian-surface (TRS) method [34,35], and from a Hartree-Fock-Bogolyubov (HFB) self-consistent mean-field approach [36]. All of these

calculations reveal that the cesium isotopes with $112 \leqslant A \leqslant 126$ are expected to have sizable ground-state quadrupole deformations. At $N = 57$, ^{112}Cs is predicted to have ground-state deformation of $\beta_2 \simeq 0.21$–0.24. Consideration of how the positions of single-particle orbitals vary with deformation suggests that, like the immediately heavier odd-odd cesium isotopes, the proton Fermi level for ^{112}Cs will lie close to the $h_{11/2}[550]1/2^-$ orbital. For neutrons, the Fermi level will lie close to the $h_{11/2}[541]3/2^-$ orbital and to the $g_{7/2}/d_{5/2}$ $[411]3/2^+$ and $[413]5/2^+$ orbitals. In the neighboring heavier odd-odd cesium isotopes, the yrast sequence is formed by the rotational band built on the $\nu(h_{11/2}) \otimes \pi(h_{11/2})$ configuration. It is possible that this is the dominant yrast configuration in ^{112}Cs; a systematic comparison of yrast bands in the neighboring odd-odd cesium isotopes has, therefore, been carried out. Figures 5(b) and 5(c) illustrate the excitation energies in ^{112}Cs in comparison to the lowest members of the even-spin [signature $\alpha = 0$; Fig. 5(b)] and odd-spin [$\alpha = 1$; Fig. 5(c)] sequences in the $\nu(h_{11/2}) \otimes \pi(h_{11/2})$ bands of $^{114-126}$Cs. For ^{114}Cs, just one sequence of $E2$ transitions was observed [22]; the same data are, therefore, given on both Figs. 5(b) and 5(c). In that case, analysis of excitation-energy systematics suggested that the observed sequence has odd spins ($\alpha = 1$). It can clearly be seen in Figs. 5(b) and 5(c) that the excitation energies vary smoothly with neutron number. If the ^{112}Cs data form a band based on the same underlying configuration, then those data are likely to continue the trend. The ^{112}Cs data, as presented in Fig. 4, appear to be in reasonable agreement with both the even- and odd-spin data, and it is, therefore, not possible to make any spin assignments based on this comparison. It is worth pointing out that, for both the even- and odd-spin cases, the positions of the ^{112}Cs states would represent a slight decrease in the energy spacings, corresponding to a larger moment of inertia and higher deformation. If confirmed, this would be in contradiction to the calculations [Fig. 5(a)] which all suggest that the deformation decreases with decreasing neutron number below $N \simeq 63$.

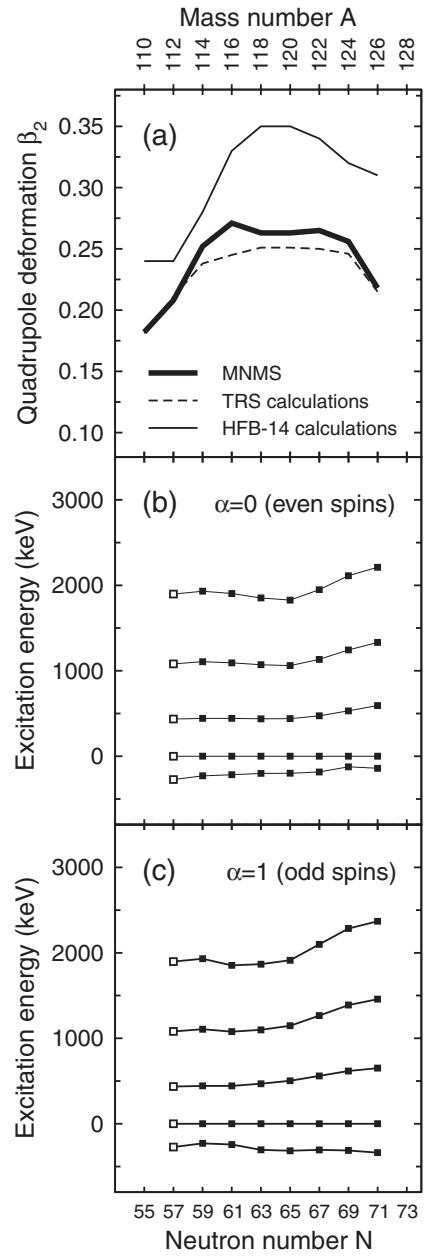

FIG. 5. Calculated quadrupole-deformation parameters β_2 and excitation-energy systematics of excited states for odd-odd cesium isotopes with $110 \leqslant A \leqslant 126$ ($55 \leqslant N \leqslant 71$). Panel (a) presents values of β_2 from the macroscopic-microscopic calculations of Möller, Nix, Myers, and Swiatecki (MNMS) [2], from TRS calculations [34,35], and from HFB self-consistent mean-field calculations [36]. Panels (b) and (c) show energies of excited states in ^{112}Cs in comparison to the $\alpha = 0$ [even spins, panel (b)] and $\alpha = 1$ [odd spins, panel (c)] sequences of $\nu(h_{11/2}) \otimes \pi(h_{11/2})$ bands in $^{114-126}$Cs. The energies are shown relative to the 10^+ [panel (b)] or 11^+ [panel (c)] state in each nucleus. The data for ^{112,114}Cs are the same in both panels; for these nuclei, only one $E2$ sequence has been observed, which has been assumed [22] to have odd spins. The data for $^{114-126}$Cs are taken from Refs. [3,17,21,22,37–41] with spin assignments from Ref. [42].

C. Aligned angular momenta

To investigate further the rotational properties of the band assigned to ^{112}Cs, its aligned angular momentum [43] has been compared to theoretical predictions and to analogous bands in neighboring nuclei. TRS calculations [34,35] were performed for all likely configurations of the valence neutron and proton. The deformations for all of the configurations were found to lie within a small range with $0.186 \leqslant \beta_2 \leqslant 0.211$, $0.033 \leqslant \beta_4 \leqslant 0.044$, and $-2^\circ \leqslant \gamma \leqslant 12^\circ$. Woods-Saxon cranked shell-model (CSM) calculations [44,45] were carried out for deformations within this range. It was found that the frequencies of alignment of the lowest pairs of quasiparticles do not vary significantly over this range, so the data can be considered using an *average* deformation. For $\beta_2 = 0.2$, $\beta_4 = 0.04$, and $\gamma = 0^\circ$, the CSM calculations predict the alignments of pairs of $h_{11/2}$ neutrons at rotational frequencies of 0.35 (EF in the usual nomenclature), 0.52 (FG), and 0.53 (EH) MeV/$\hbar$.

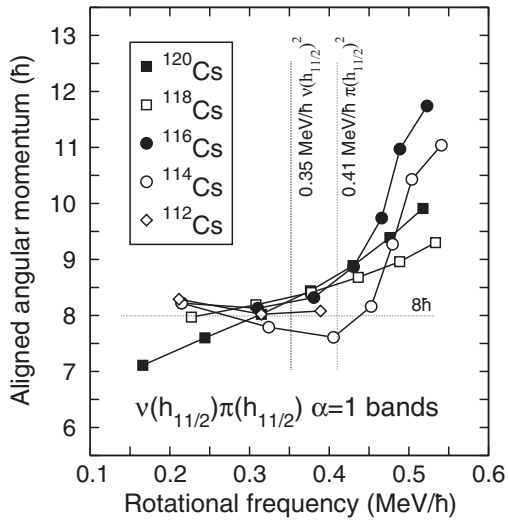

FIG. 6. Aligned angular momenta of the $\nu(h_{11/2}) \otimes \pi(h_{11/2})$ odd-spin ($\alpha = 1$) bands in ^{112,114,116,118,120}Cs. The data for ^{114,116,118,120}Cs are taken from Refs. [3,17,21,22]. For all data points, a reference configuration with the Harris parameters [46] $\mathcal{J}_0 = 17.0$ MeV^{-1} $\hbar^2$ and $\mathcal{J}_1 = 25.8$ MeV^{-3} $\hbar^4$ [47] has been subtracted. A value of $K = 3$ has been assumed for all of the bands. The initial value of the aligned angular momentum ($\sim 8\,\hbar$) and the CSM-predicted $\nu(h_{11/2})^2$ (EF) and $\pi(h_{11/2})^2$ (ef) alignment frequencies for ^{112}Cs are marked.

The alignments of $h_{11/2}$ protons are predicted to occur at 0.41 (ef), 0.62 (fg), and 0.64 (eh) MeV/$\hbar$. The alignments of pairs of positive-parity neutrons (AB) and protons (ab) (from the $g_{7/2}$ and $d_{5/2}$ subshells) are predicted to occur above 0.65 MeV/$\hbar$. The aligned angular momentum of the ^{112}Cs band is presented in Fig. 6 in comparison with odd-spin sequences of the $\nu(h_{11/2}) \otimes \pi(h_{11/2})$ bands in ^{114,116,118,120}Cs [3,17,21,22]. The CSM-predicted positions of the first $h_{11/2}$ neutron (EF) and proton (ef) alignments at 0.35 and 0.41 MeV/$\hbar$, respectively, are marked on the figure. For ^{112}Cs, the alignment predicted at 0.35 MeV/$\hbar$ is not observed and, although the data do not extend beyond a rotational frequency of $\sim$0.37 MeV/$\hbar$, there is no evidence for the onset of an upbend or backbend at 0.41 MeV/$\hbar$. The non-observation of these alignments is consistent with the assignment of a $\nu(h_{11/2}) \otimes \pi(h_{11/2})$ configuration underlying the ^{112}Cs states, for which both of the first $h_{11/2}$ alignments would be blocked. The upbend observed at around 0.47 MeV/$\hbar$ in ^{114,116}Cs is assigned to the second $h_{11/2}$ neutron (FG) alignment; this alignment is predicted to occur at 0.52 MeV/$\hbar$ in ^{112}Cs. It would be very interesting to extend the data to higher spins to look for evidence of this alignment.

V. SUMMARY

In summary, excited states have been observed for the first time in the very neutron-deficient $N = Z + 2$ ^{112}Cs isotope. Five γ-ray transitions have been assigned to ^{112}Cs by their correlation with characteristic ^{112}Cs proton decays, using the method of recoil-decay tagging. The observed γ rays have been arranged into a level scheme on the basis of intensity measurements and the systematics of excitation energies of the neighboring odd-odd cesium isotopes. Given the proposed level scheme, the data show no evidence for the $\nu(h_{11/2})^2$ or $\pi(h_{11/2})^2$ alignments, which are predicted to occur, or begin, within the observable range of rotational frequencies. This non-observation is consistent with an underlying $\nu(h_{11/2}) \otimes \pi(h_{11/2})$ assignment. Furthermore, the spacing of levels appears to decrease in ^{112}Cs, compared to the heavier odd-odd cesium isotopes, implying a larger moment of inertia and larger deformation. This is in contradiction to various predictions which all suggest the deformation should decrease with decreasing N in this region. Some evidence has been obtained for a second proton-decay branch in ^{112}Cs with proton energy 710(20) keV and half-life 170^{+50}_{-30} μs. Due to low counts and large uncertainties, it is not possible to draw any definite conclusion based on this tentative second ^{112}Cs decay. However, further investigation of this decay could provide valuable information about the single-particle states in the daughter nucleus ^{111}Xe.

ACKNOWLEDGMENTS

This work is supported in part by the NSF, the EPSRC/STFC (UK), and by the Department of Energy, Office of Nuclear Physics, under contract numbers DE-AC02-06CH11357 (ANL) and DE-FG02-88ER-40406 (Washington University). J.F.S. acknowledges support from the Scottish Universities Physics Alliance.

[1] P. J. Woods and C. N. Davids, Annu. Rev. Nucl. Part. Sci. **47**, 541 (1997).
[2] P. Möller, J. R. Nix, W. D. Myers, and W. J. Swiatecki, At. Data Nucl. Data Tables **59**, 185 (1995).
[3] J. F. Smith, C. J. Chiara, D. B. Fossan, G. R. Gluckman, G. J. Lane, J. M. Sears, I. Thorslund, H. Amro, C. N. Davids, R. V. F. Janssens, D. Seweryniak, I. M. Hibbert, R. Wadsworth, I. Y. Lee, and A. O. Macchiavelli, Phys. Lett. B **406**, 7 (1997).
[4] J. F. Smith, V. Medina-Chico, C. J. Chiara, D. B. Fossan, G. J. Lane, J. M. Sears, I. Thorslund, H. Amro, C. N. Davids, R. V. F. Janssens, D. Seweryniak, I. M. Hibbert, R. Wadsworth, I. Y. Lee, and A. O. Macchiavelli, Phys. Rev. C **63**, 024319 (2001).
[5] W. Satuła, R. Wyss, and F. Dönau, Nucl. Phys. A **565**, 573 (1993).
[6] E. S. Paul *et al.*, Phys. Rev. C **51**, 78 (1995).
[7] D. Schardt, R. Kirchner, O. Klepper, W. Reisdorf, E. Roeckl, P. Tidemand-Petersson, G. T. Ewan, E. Hagberg, B. Jonson, S. Mattsson, and G. Nyman, Nucl. Phys. A **326**, 65 (1979).
[8] D. Schardt, T. Batsch, R. Kirchner, O. Klepper, W. Kurcewicz, E. Roeckl, and P. Tidemand-Petersson, Nucl. Phys. A **368**, 153 (1981).
[9] T. Faestermann, A. Gillitzer, K. Hartel, P. Kienle, and E. Nolte, Phys. Lett. B **137**, 23 (1984).
[10] B. Hadinia *et al.*, Phys. Rev. C **72**, 041303(R) (2005).

[11] B. Hadinia *et al.*, Phys. Rev. C **70**, 064314 (2004).
[12] C.-H. Yu, A. Galindo-Uribarri, S. D. Paul, M. P. Carpenter, C. N. Davids, R. V. F. Janssens, C. J. Lister, D. Seweryniak, J. Uusitalo, and B. D. MacDonald, Phys. Rev. C **59**, R1834 (1999).
[13] M. Petri *et al.*, Phys. Rev. C **76**, 054301 (2007).
[14] M. Sandzelius *et al.*, Phys. Rev. Lett. **99**, 022501 (2007).
[15] C.-H. Yu, J. C. Batchelder, C. R. Bingham, C. J. Gross, R. Grzywacz, and K. Rykaczewski, in *Proceedings of Proton Emitting Nuclei: Second International Symposium; PROCON 2003*, Legnaro, Italy, CP 681, edited by E. Maglione and F. Soramel (AIP, New York, 2003), p. 172.
[16] R. D. Page, P. J. Woods, R. A. Cunningham, T. Davinson, N. J. Davis, A. N. James, K. Livingston, P. J. Sellin, and A. C. Shotter, Phys. Rev. Lett. **72**, 1798 (1994).
[17] B. Cederwall, F. Liden, A. Johnson, L. Hildingsson, R. Wyss, B. Fant, S. Juutinen, P. Ahonen, S. Mitarai, J. Mukai, J. Nyberg, I. Ragnarsson, and P. B. Semmes, Nucl. Phys. A **542**, 454 (1992).
[18] C.-B. Moon, S. J. Chae, J. H. Ha, T. Komatsubara, Y. Sasaki, T. Jumatsu, K. Yamada, K. Satou, and K. Furuno, Nucl. Phys. A **696**, 45 (2001).
[19] A. B. Kamdar, M.Sc. thesis, University of Manchester (2003).
[20] J. F. Smith, C. L. Wilson, A. B. Kamdar, C. J. Chiara, M. P. Carpenter, C. N. Davids, M. Devlin, D. B. Fossan, S. J. Freeman, R. V. F. Janssens, D. R. LaFosse, D. G. Sarantites, D. Seweryniak, K. Starosta, R. Wadsworth, and A. N. Wilson (to be published).
[21] J. F. Smith, C. J. Chiara, M. P. Carpenter, C. N. Davids, M. Devlin, D. B. Fossan, S. J. Freeman, R. V. F. Janssens, D. R. LaFosse, D. G. Sarantites, D. Seweryniak, K. Starosta, R. Wadsworth, A. N. Wilson, and R. Wyss, Phys. Rev. C **74**, 034310 (2006).
[22] J. F. Smith *et al.*, Phys. Rev. C **73**, 061303(R) (2006).
[23] R. V. F. Janssens and F. S. Stephens, Nucl. Phys. News **6**, 9 (1996).
[24] P. J. Nolan, F. A. Beck, and D. B. Fossan, Annu. Rev. Nucl. Part. Sci. **44**, 561 (1994).
[25] Cary N. Davids and James D. Larson, Nucl. Instrum. Methods B **40/41**, 1224 (1989).
[26] C. N. Davids, B. B. Back, K. Bindra, D. J. Henderson, W. Kutschera, T. Lauritsen, Y. Nagame, P. Sugathan, A. V. Ramayya, and W. B. Walters, Nucl. Instrum. Methods B **70**, 358 (1992).
[27] D. C. Radford, Nucl. Instrum. Methods A **361**, 297 (1995); Nucl. Instrum. Meth. Phys. Res. A **361**, 306 (1995).
[28] A. G. Smith (private communication).
[29] K.-H. Schmidt, C.-C. Sahm, K. Pielenz, and H.-G. Clerc, Z. Phys. A **316**, 19 (1984).
[30] W. J. McBride, IEEE Trans. Nucl. Sci. **15**, 350 (1968).
[31] D. Seweryniak, K. Starosta, C. N. Davids, S. Gros, A. A. Hecht, N. Hoteling, T. L. Khoo, K. Lagergren, G. Lotay, D. Peterson, A. Robinson, C. Vaman, W. B. Walters, P. J. Woods, and S. Zhu, Phys. Rev. C **73**, 061301(R) (2006).
[32] I. G. Darby, R. K. Grzywacz, J. C. Batchelder, C. R. Bingham, L. Cartegni, C. J. Gross, M. Hjorth-Jensen, D. T. Joss, S. N. Liddick, W. Nazarewicz, S. Padgett, R. D. Page, T. Papenbrock, M. M. Rajabali, J. Rotureau, and K. P. Rykaczewski, Phys. Rev. Lett. **105**, 162502 (2010).
[33] L. S. Ferreira and E. Maglione, Phys. Rev. Lett. **86**, 1721 (2001).
[34] R. Wyss, J. Nyberg, A. Johnson, R. Bengtsson, and W. Nazarewicz, Phys. Lett. B **215**, 211 (1988).
[35] W. Nazarewicz, R. Wyss, and A. Johnson, Nucl. Phys. A **503**, 285 (1989).
[36] http://www-astro.ulb.ac.be/Html/hfb14.html.
[37] J. F. Smith, C. J. Chiara, D. B. Fossan, G. J. Lane, J. F. Lewicki, J. M. Sears, and P. Vaska, Phys. Rev. C **58**, 3237 (1998).
[38] Jingbin Lu, Yunzuo Liu, Lichang Yin, Guangyi Zhao, Fan Zhang, Xianfeng Li, Rui Meng, Zhongwen Wang, Yingjun Ma, Zhikui Wang, Junde Huo, Xiaoguang Wu, Shuxian Wen, Guangsheng Li, and Chunxiang Yang, Phys. Rev. C **62**, 057304 (2000).
[39] A. Gizon, J. Timár, J. Gizon, B. Weiss, D. Barnéoud, C. Foin, J. Genevey, F. Hannachi, C. F. Liang, A. Lopez-Martens, P. Paris, B. M. Nyakó, L. Zolnai, J. C. Merdinger, S. Brant, and V. Paar, Nucl. Phys. A **694**, 63 (2001).
[40] Shouyu Wang, Yunzuo Liu, Yingjun Ma, T. Komatsubara, and Yuhu Zhang, Phys. Rev. C **75**, 037302 (2007).
[41] T. Komatsubara, K. Furuno, T. Hosoda, J. Mukai, T. Hayakawa, T. Morikawa, Y. Iwata, N. Kato, J. Espino, J. Gascon, N. Gjørup, G. B. Hagemann, H. J. Jensen, D. Jerrestam, J. Nyberg, G. Sletten, B. Cederwall, and P. O. Tjøm, Nucl. Phys. A **557**, 419c (1993).
[42] Yunzuo Liu, Jingbin Lu, Yingjun Ma, Guangyi Zhao, Hua Zheng, and Shangui Zhou, Phys. Rev. C. **58**, 1849 (1998).
[43] R. Bengtsson, S. Frauendorf, and F.-R. May, At. Data Nucl. Data Tables **35**, 15 (1986).
[44] W. Nazarewicz, J. Dudek, R. Bengtsson, T. Bengtsson, and I. Ragnarsson, Nucl. Phys. A **435**, 397 (1985).
[45] S. Cwiok, J. Dudek, W. Nazarewicz, J. Skalski, and T. Werner, Comp. Phys. Comm. **46**, 379 (1987).
[46] Samuel M. Harris, Phys. Rev. **138**, B509 (1965).
[47] D. M. Todd, R. Aryaeinejad, D. J. G. Love, A. H. Nelson, P. J. Nolan, P. J. Smith, and P. J. Twin, J. Phys. G **10**, 1407 (1984).